



**Addressing transcranial electrical stimulation variability through prospective individualized dosing of electric field strength in 300 participants across two samples the 2-SPED approach**

**Van Hoornweder, Sybren; Caulfield, Kevin A.; Nitsche, Michael; Thielscher, Axel; Meesen, Raf L.J.**

*Published in:*  
Journal of Neural Engineering

*Link to article, DOI:*  
[10.1088/1741-2552/ac9a78](https://doi.org/10.1088/1741-2552/ac9a78)

*Publication date:*  
2022

*Document Version*  
Publisher's PDF, also known as Version of record

[Link back to DTU Orbit](#)

*Citation (APA):*  
Van Hoornweder, S., Caulfield, K. A., Nitsche, M., Thielscher, A., & Meesen, R. L. J. (2022). Addressing transcranial electrical stimulation variability through prospective individualized dosing of electric field strength in 300 participants across two samples: the 2-SPED approach. *Journal of Neural Engineering*, 19(5), Article 056045. <https://doi.org/10.1088/1741-2552/ac9a78>

---

**General rights**

Copyright and moral rights for the publications made accessible in the public portal are retained by the authors and/or other copyright owners and it is a condition of accessing publications that users recognise and abide by the legal requirements associated with these rights.

- Users may download and print one copy of any publication from the public portal for the purpose of private study or research.
- You may not further distribute the material or use it for any profit-making activity or commercial gain
- You may freely distribute the URL identifying the publication in the public portal

If you believe that this document breaches copyright please contact us providing details, and we will remove access to the work immediately and investigate your claim.



## PAPER

## OPEN ACCESS





RECEIVED  
10 May 2022REVISED  
13 October 2022ACCEPTED FOR PUBLICATION  
14 October 2022PUBLISHED  
28 October 2022

Original content from this work may be used under the terms of the [Creative Commons Attribution 4.0 licence](#).

Any further distribution of this work must maintain attribution to the author(s) and the title of the work, journal citation and DOI.



# Addressing transcranial electrical stimulation variability through prospective individualized dosing of electric field strength in 300 participants across two samples: the 2-SPED approach

Sybren Van Hoornweder<sup>1,\*</sup> , Kevin A Caulfield<sup>2</sup> , Michael Nitsche<sup>3,4</sup>, Axel Thielscher<sup>5,6</sup>   
and Raf L J Meesen<sup>1,7</sup> 

<sup>1</sup> REVAL—Rehabilitation Research Center, Faculty of Rehabilitation Sciences, University of Hasselt, Diepenbeek, Belgium

<sup>2</sup> Brain Stimulation Laboratory, Department of Psychiatry, Medical University of South Carolina, Charleston, SC, United States of America

<sup>3</sup> Department of Psychology and Neurosciences, Leibniz Research Centre for Working Environment and Human Factors, Dortmund, Germany

<sup>4</sup> Department of Neurology, University Medical Hospital Bergmannsheil, Bürkle de la Camp-Platz, Bochum, Germany

<sup>5</sup> Section for Magnetic Resonance, Department of Health Technology, Technical University of Denmark, Kgs Lyngby, Denmark

<sup>6</sup> Danish Research Centre for Magnetic Resonance, Centre for Functional and Diagnostic Imaging and Research, Copenhagen University Hospital Amager and Hvidovre, Copenhagen, Denmark

<sup>7</sup> Movement Control and Neuroplasticity Research Group, Department of Movement Sciences, Group Biomedical Sciences KU Leuven, Leuven, Belgium

\* Author to whom any correspondence should be addressed.

E-mail: [Sybren.vanhoornweder@uhasselt.be](mailto:Sybren.vanhoornweder@uhasselt.be)

**Keywords:** electric field (E-field) modeling, transcranial electrical stimulation (tES), transcranial direct current stimulation (tDCS), finite element method (FEM), noninvasive brain stimulation, computational dosimetry

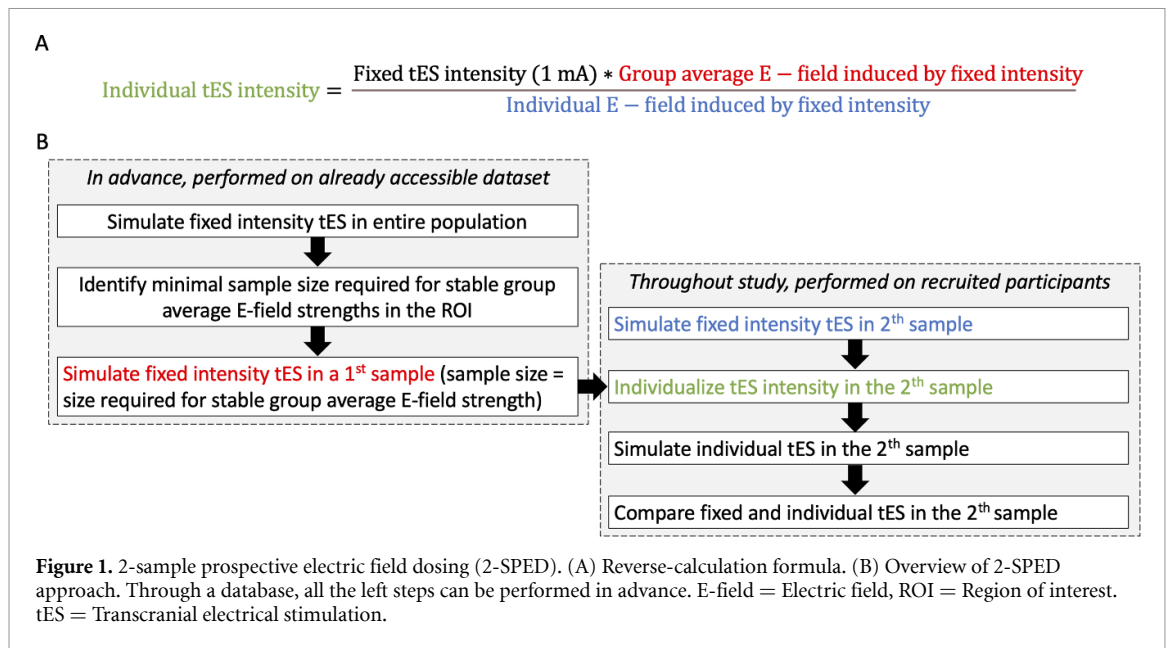
## Abstract

**Objective.** Transcranial electrical stimulation (tES) is a promising method for modulating brain activity and excitability with variable results to date. To minimize electric (E-)field strength variability, we introduce the 2-sample prospective E-field dosing (2-SPED) approach, which uses E-field strengths induced by tES in a first population to individualize stimulation intensity in a second population. **Approach.** We performed E-field modeling of three common tES montages in 300 healthy younger adults. First, permutation analyses identified the sample size required to obtain a stable group average E-field in the primary motor cortex (M1), with stability being defined as the number of participants where all group-average E-field strengths  $\pm$  standard deviation did not leave the population's 5–95 percentile range. Second, this stable group average was used to individualize tES intensity in a second independent population ( $n = 100$ ). The impact of individualized versus fixed intensity tES on E-field strength variability was analyzed. **Main results.** In the first population, stable group average E-field strengths (V/m) in M1 were achieved at 74–85 participants, depending on the tES montage. Individualizing the stimulation intensity (mA) in the second population resulted in uniform M1 E-field strength (all  $p < 0.001$ ) and significantly diminished peak cortical E-field strength variability (all  $p < 0.01$ ), across all montages. **Significance.** 2-SPED is a feasible way to prospectively induce more uniform E-field strengths in a region of interest. Future studies might apply 2-SPED to investigate whether decreased E-field strength variability also results in decreased physiological and behavioral variability in response to tES.

## 1. Introduction

Transcranial electrical stimulation (tES) is a form of noninvasive brain stimulation that propagates low intensity electrical currents through the brain, via electrodes placed on the scalp [1]. Although the

electric (E-)fields generated by tES are generally too low to elicit neuronal firing, they can modulate neuronal excitability and/or entrain neuronal firing [1–4]. As a result of its ease of use, cost-effectiveness and portability, tES has become increasingly popular as both a fundamental tool to investigate the



neurophysiological foundation of psychological processes, and a potential clinical therapy that promises to alter cognitive and motor behavior [5]. Although a large body of evidence has previously demonstrated the potential of tES, widely variable results present a major hurdle for routine implementation, as they give rise to small effect sizes and ambiguous conclusions [6, 7].

Per standard, tES protocols apply a fixed current intensity to each person, irrespective of individual head anatomy. However, intracranially validated modeling studies have revealed that anatomical idiosyncrasies give rise to E-field strength variations of up to 100% across persons. As the E-field generated in the brain is a cardinal physical agent of tES [8–17], next to other factors such as current direction [18], this shortcoming could account for a large part of the widely variable effects observable in tES.

In an effort to reduce E-field strength variability across persons, a reverse-calculation method based on computational modeling dosimetry has been proposed (figure 1(A)) [13, 19–21]. This method uses the simulated E-field strength induced by fixed intensity tES in one person and on average in a group to calculate an individual stimulation intensity per person. Applying tES with this individual intensity results in uniform E-field strengths across all persons.

Although theoretically appealing, the reverse-calculation method has not yet been implemented *in-vivo*. Likely, this is due to the limiting step of determining an (average) E-field intensity to base the reverse-calculation dosing on. To date, there is not yet a consensus reached on whether there is an optimal E-field strength for dosing. Some researchers have aimed to answer this question by retrospectively determining an optimal E-field strength, but conflicting results impede unambiguous interpretation

[12, 13, 15, 22]. A parallel method we propose here is to use the group average E-field induced by fixed intensity tES in a large first sample (S1) as a guide for reverse-calculation intensity dosing in a second sample (S2) (figure 1(B)). As such, we established a 2-Sample Prospective E-field Dosing (2-SPED) method. Moreover, to the best of our knowledge, the reverse-calculation method has not yet been investigated in several tES montages such as high-definition  $4 \times 1$  tES and center-surround ring tES, despite the fact that these montages have been used in a vast array of protocols due to the presumed higher spatial focality of the E-field produced by these montages [23–25].

In summary, we aim to conceptualize and validate the 2-SPED approach in three tES montages. By leveraging the extensive Human Connectome Project MRI dataset, we can include a large number of participants to capture a wide range of anatomical idiosyncrasies. We hypothesize that the 2-SPED approach will significantly reduce peak and average ROI E-field strength variability [13].

## 2. Methods

### 2.1. Participants

In total, 300 healthy participants (150 men and 150 women) were included [26]. Inclusion criteria were persons aged 22–35 years old, Mini Mental Status Exam score  $\geq 29$ , and no history of psychiatric disorder, substance abuse, neurological and/or cardiovascular disease. Exclusion criteria were  $\geq 2$  seizures in one's lifetime, genetic disorders, migraine medication use in the past year, head injuries, premature birth, pregnancy, unsafe (metal) device in the body, and/or chemotherapy. The study was approved by the local ethical committee of Hasselt (approval number:

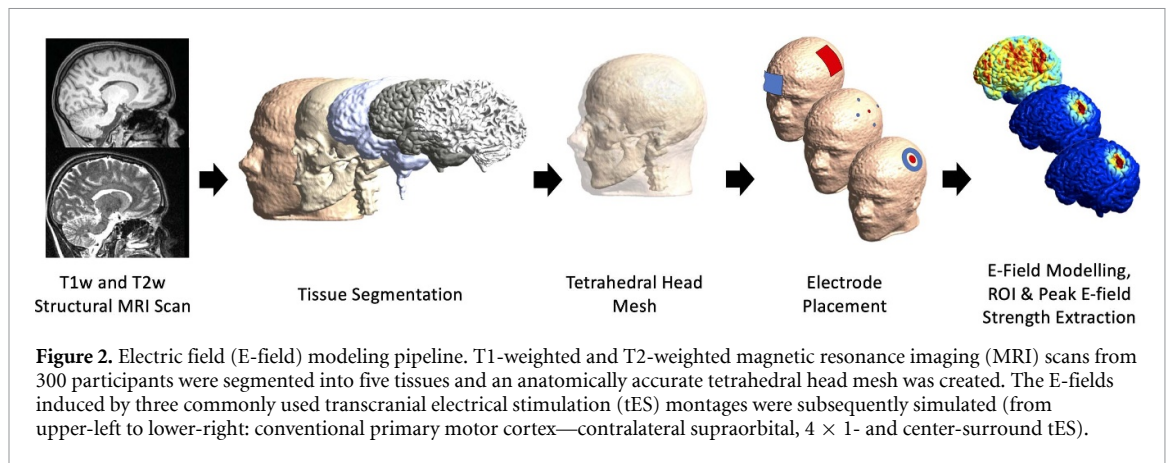


**Figure 2.** Electric field (E-field) modeling pipeline. T1-weighted and T2-weighted magnetic resonance imaging (MRI) scans from 300 participants were segmented into five tissues and an anatomically accurate tetrahedral head mesh was created. The E-fields induced by three commonly used transcranial electrical stimulation (tES) montages were subsequently simulated (from upper-left to lower-right: conventional primary motor cortex—contralateral supraorbital,  $4 \times 1$ - and center-surround tES).

CME2022/011) and was in line with the Declaration of Helsinki and its amendments.

## 2.2. Computational modeling

In line with our previous work [27, 28], anatomical T1-weighted and T2-weighted MRI-scans were acquired with the Siemens MAGNETOM 3 T scanner (32-channel head coil). T1-weighted scans were acquired with the following parameters: TR = 2400 ms, TE = 2.14 ms, flip angle =  $8^\circ$ , field of view =  $224 \times 224 \times 180$  mm, voxel size =  $0.7 \text{ mm}^3$ . T2-weighted scans were acquired with the following parameters: TR = 3200 ms, TE = 565 ms, field of view =  $224 \times 224 \times 180$  mm, voxel size =  $0.7 \text{ mm}^3$ . MRI-scans were used to construct tetrahedral head meshes for use in E-field calculations based on the finite element method. Head model reconstruction was performed via the headreco command [29], which uses SPM12 [30] and CAT12 [31]. All head models were visually inspected to ensure accurate segmentation of the skin, bone, cerebrospinal fluid, grey matter, white matter, and eyes (figure 2). As a result of this inspection, 11 participants (6 males, 5 females) were excluded due to intersecting tissue layers, resulting in a final sample size of 289 participants.

## 2.3. Transcranial electrical stimulation

Three commonly used tES montages (figure 2) were simulated in SimNIBS (v3.2.3), which has been validated against intracranial recordings and other modeling software packages [32–34]. Conventional primary motor cortex (M1)—contralateral supraorbital (SO) tES consisted of two rectangular electrodes ( $4 \times 5$  cm) placed over C3 and FP2 (supraorbital area). The  $4 \times 1$  montage consisted of a circular anode over C3 and four circular cathodes over FC3, C1, CP3 and C5 (0.25 cm electrode radius). Center-surround tES consisted of a circular anode (1 cm electrode radius) and a ring cathode over C3 (2 cm inner radius, 3 cm outer radius).

All montages were simulated in SimNIBS at an intensity of 1 mA. For the  $4 \times 1$  montage, this meant that the intensity of each cathode

was 0.25 mA. The following conductivities were assigned to each tissue:  $\sigma_{\text{white matter}} = 0.126 \text{ S/m}$ ,  $\sigma_{\text{grey matter}} = 0.275 \text{ S/m}$ ,  $\sigma_{\text{cerebrospinal fluid}} = 1.654 \text{ S/m}$ ,  $\sigma_{\text{bone}} = 0.01 \text{ S/m}$ ,  $\sigma_{\text{skin}} = 0.465 \text{ S/m}$ ,  $\sigma_{\text{eyes}} = 0.5 \text{ S/m}$ ,  $\sigma_{\text{electrode rubber}} = 29.4 \text{ S/m}$ ,  $\sigma_{\text{electrode gel}} = 1 \text{ S/m}$  [35–37]. Next, E-fields in the ROI were extracted per montage and participant. The ROI was defined as a 10 mm radius sphere with the peak MNI coordinate of M1 ( $x = -37$ ,  $y = -21$ ,  $z = 58$ ) transformed to subject space serving as the center point [38]. Coordinate transformation from MNI to subject space was done using the mni2subject\_coord command [34].

## 2.4. Stability of a group average E-field strength in subsample 1

The current approach was based on the work of Schönbrodt and Perugini [39]. The number of participants required to achieve a stable group average E-field measure for each tES montage was calculated using bootstrapped statistics in MATLAB R2021a (The Mathworks, Inc., Natick, Massachusetts, United States). Subsamples with increasing size from 5 to 289 were randomly selected from the entire sample. The group average E-field of each subsample was calculated. This procedure was repeated 10,000 times per subsample size. Next, the 5th and 95th percentile of the entire sample was calculated, this range was defined as the corridor of stability. The subsample size at which all the group average E-field strengths  $\pm$  the respective standard deviation of the subsample fell within the corridor of stability and never left it at increasing subsample sizes was defined as the point of stability. The most conservative point of stability across the 3 tES montages was used as sample size for S1. In S1, we then extracted the group average E-field strength in the ROI induced by each tES montage.

## 2.5. Testing transcranial electrical stimulation individualization in an independent subsample 2

Subsequently, 100 participants (non-overlapping with S1) were assigned to S2. Per tES montage,

the group average E-field strength in the ROI of S1 was multiplied with 1 mA (i.e. the used tES intensity) (figure 1(A)). For each S2-participant and tES montage, this value was divided by the individual E-field strength induced in the ROI by the respective tES montage at an intensity of 1 mA. This resulted in an individual stimulation intensity per S2-participant and tES montage. All simulations were re-conducted using the individual stimulation intensity.

In total, 600 E-field models were calculated (3 tES montages \* 2 stimulation intensities \* 100 S2-participants). Per model, the average E-field strength induced in M1 and robust peak E-field strength, defined as the 99th percentile of the total induced cortical E-field strength, were extracted for analyses. Inclusion of peak E-field strength gives additional information regarding the validity of 2-SPED, given that this value is not directly influenced by the reverse-calculation approach, in contrast to the average E-field strength in the ROI.

## 2.6. Statistical analyses

R (R Foundation for Statistical Computing, Vienna, Austria) and RStudio (RStudio Team, Boston, Massachusetts, United States) were used for the statistical analyses [40, 41]. Descriptive statistics (average, standard deviation, variation coefficient [VC], minimum, maximum and range) were calculated to examine E-field strength induced by fixed and individual intensity tES. Moreover, differences in ROI and peak E-field variability between fixed versus individual tES were inspected through inferential statistics. To this end, the modified Pitman–Morgan test, a pairwise test based on Spearman’s rank correlations instead of Pearson’s R correlations, was used [42]. This modified test was used due to its superior robustness against Type 1 errors in case of deviation from normality. The significance level was set to  $\alpha = 0.05$ .

## 3. Results

Results are noted as average  $\pm$  standard deviation unless stated otherwise.

### 3.1. Stability analyses

In line with figure 3, conventional M1-SO tES required a sample size of 74 participants to achieve a stable group-average E-field strength. For the  $4 \times 1$  tES montage, the point of stability was achieved at 85 participants. Using center-surround tES, the point of stability was achieved at 75 participants. As such, S1 consisted of 85 participants. The group average ROI E-field strength induced in S1 was 0.110 V/m for conventional tES, 0.079 V/m for  $4 \times 1$  tES and 0.035 V/m for center-surround tES. These group averages were used for intensity individualization in S2.

### 3.2. Fixed versus individual transcranial electrical stimulation intensity in an independent subsample 2

In S2, individual stimulation intensity to match the group average ROI E-field strengths from S1 ranged between 0.549–1.498 mA (Conventional M1-SO tES), 0.309–2.307 mA ( $4 \times 1$  tES) and 0.331–2.190 mA (Center-surround tES) (tables 1 and 2). In figure 4, we compared the E-fields produced by the individual stimulation intensity to the fixed stimulation intensity at 1 mA. Visually, fixed intensity tES induces highly variable E-field strengths across participants, while individual intensity tES effectively eliminates these variations. Although not within the scope of the current work, figure 4 also suggests that the focality of the induced E-fields became more similar across participants.

### 3.3. Conventional transcranial electrical stimulation

While fixed tES induced an E-field strength of  $0.112 \pm 0.020$  V/m in the ROI, individualized tES induced an E-field strength of  $0.110 \pm 0$  V/m. Variability in ROI E-field strength induced by fixed tES (VC = 17.54%, range = 0.128 V/m) was significantly higher than variability induced by individualized tES (VC = 0%, range = 0 V/m),  $r_{98} = 1$ ,  $p < 0.001$  (figure 5).

Peak E-field strength induced by fixed and individual tES was  $0.208 \pm 0.029$  V/m and  $0.206 \pm 0.019$  V/m, respectively. Variation in peak E-field strength induced by fixed tES (VC = 14.16%, range = 0.193 V/m) was significantly higher than variation induced by individualized tES (VC = 9.36%, range = 0.087 V/m),  $r_{98} = 0.26$ ,  $p = 0.009$  (figure 5).

### 3.4. $4 \times 1$ transcranial electrical stimulation

Fixed tES induced an E-field strength of  $0.080 \pm 0.027$  V/m in M1, while individualized tES induced an E-field strength of  $0.079 \pm 0$  V/m. Variation in M1 E-field strength induced by fixed tES (VC = 33.96%, range = 0.221 V/m) was significantly higher than variation induced by individualized tES (VC = 0%, range = 0 V/m),  $r_{98} = 1$ ,  $p < 0.001$  (figure 5).

Peak E-field strength induced by fixed and individualized tES were  $0.094 \pm 0.031$  V/m and  $0.092 \pm 0.007$  V/m, respectively. Variation was significantly higher as a result of fixed tES (VC = 32.85%, range = 0.212 V/m) versus individualized tES (VC = 7.46%, range = 0.033 V/m),  $r_{98} = 0.86$ ,  $p < 0.001$  (figure 5).

### 3.5. Center-surround transcranial electrical stimulation

Fixed tES-induced E-field strength was  $0.038 \pm 0.013$  V/m in the ROI, while individualized tES induced an average E-field strength

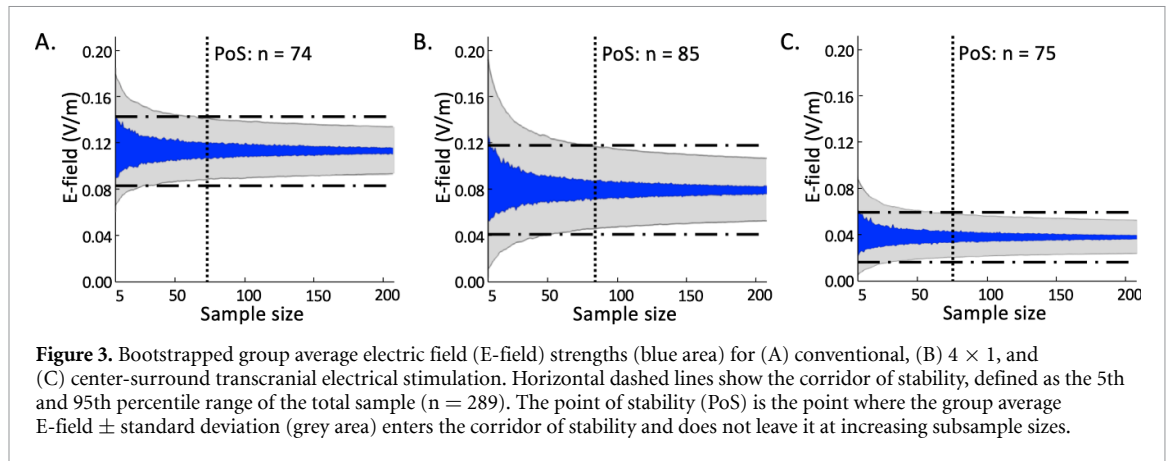


**Figure 3.** Bootstrapped group average electric field (E-field) strengths for (A) conventional, (B)  $4 \times 1$ , and (C) center-surround transcranial electrical stimulation. Horizontal dashed lines show the corridor of stability, defined as the 5th and 95th percentile range of the total sample ( $n = 289$ ). The point of stability (PoS) is the point where the group average E-field  $\pm$  standard deviation (grey area) enters the corridor of stability and does not leave it at increasing subsample sizes.

**Table 1.** Electric fields strength induced in the region of interest (the primary motor cortex, M1).

Montage	tES intensity (mA)	Average $\pm$ SD (V/m)	Variance coefficient (%)	Minimum (V/m)	Maximum (V/m)
Conventional	Fixed (1)	$0.112 \pm 0.020$	17.54	0.072	0.200
	Individual (0.549–1.498)	$0.110 \pm 0.00$	0.00	0.110	0.110
$4 \times 1$ tES	Fixed (1)	$0.080 \pm 0.027$	33.96	0.034	0.255
	Individual (0.309–2.307)	$0.079 \pm 0.00$	0.00	0.079	0.079
Center-surround tES	Fixed (1)	$0.038 \pm 0.013$	33.54	0.016	0.105
	Individual (0.331–2.190)	$0.035 \pm 0.00$	0.00	0.035	0.035

SD = standard deviation, SO = contralateral supraorbital area, tES = transcranial electrical stimulation.

**Table 2.** Peak cortical electric fields strength.

Montage	tES intensity (mA)	Average $\pm$ SD (V/m)	Variance coefficient (%)	Minimum (V/m)	Maximum (V/m)
Conventional	Fixed (1)	$0.208 \pm 0.029$	14.16	0.145	0.338
	Individual (0.549–1.498)	$0.206 \pm 0.019$	9.36	0.164	0.251
$4 \times 1$ tES	Fixed (1)	$0.094 \pm 0.031$	32.85	0.038	0.250
	Individual (0.309–2.307)	$0.092 \pm 0.007$	7.46	0.077	0.110
Center-surround tES	Fixed (1)	$0.043 \pm 0.014$	32.49	0.016	0.091
	Individual (0.331–2.190)	$0.040 \pm 0.003$	8.61	0.030	0.049

M1 = primary motor cortex, SD = standard deviation, SO = contralateral supraorbital area, tES = transcranial electrical stimulation.

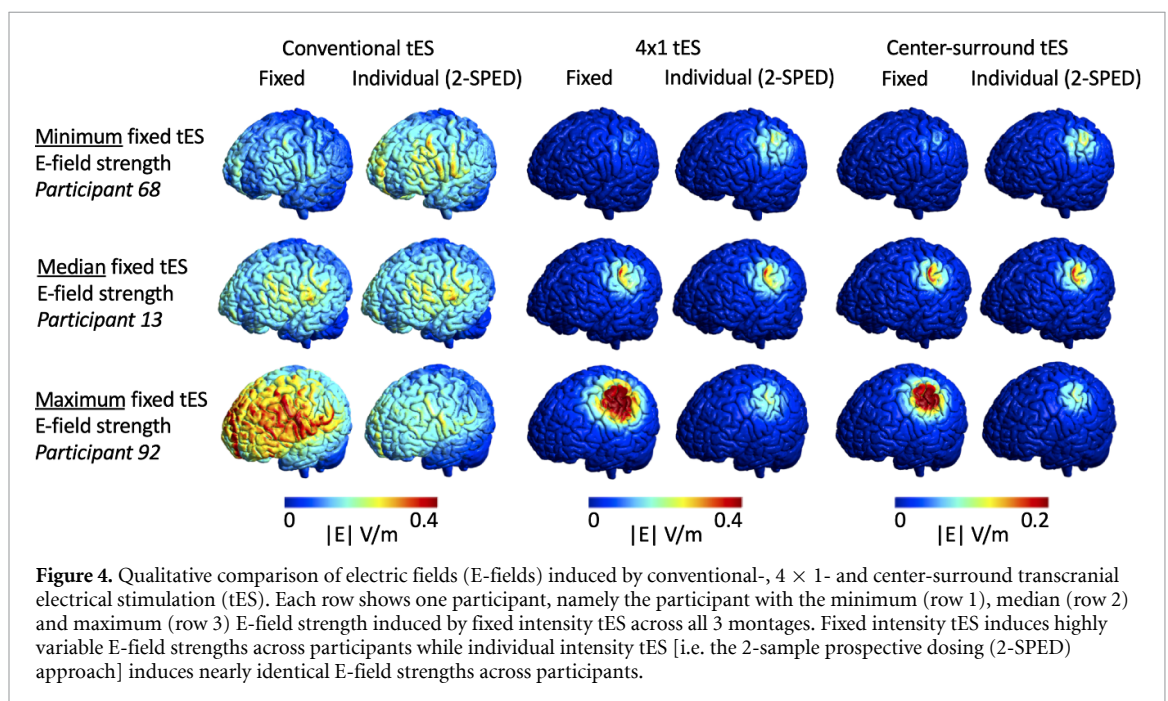
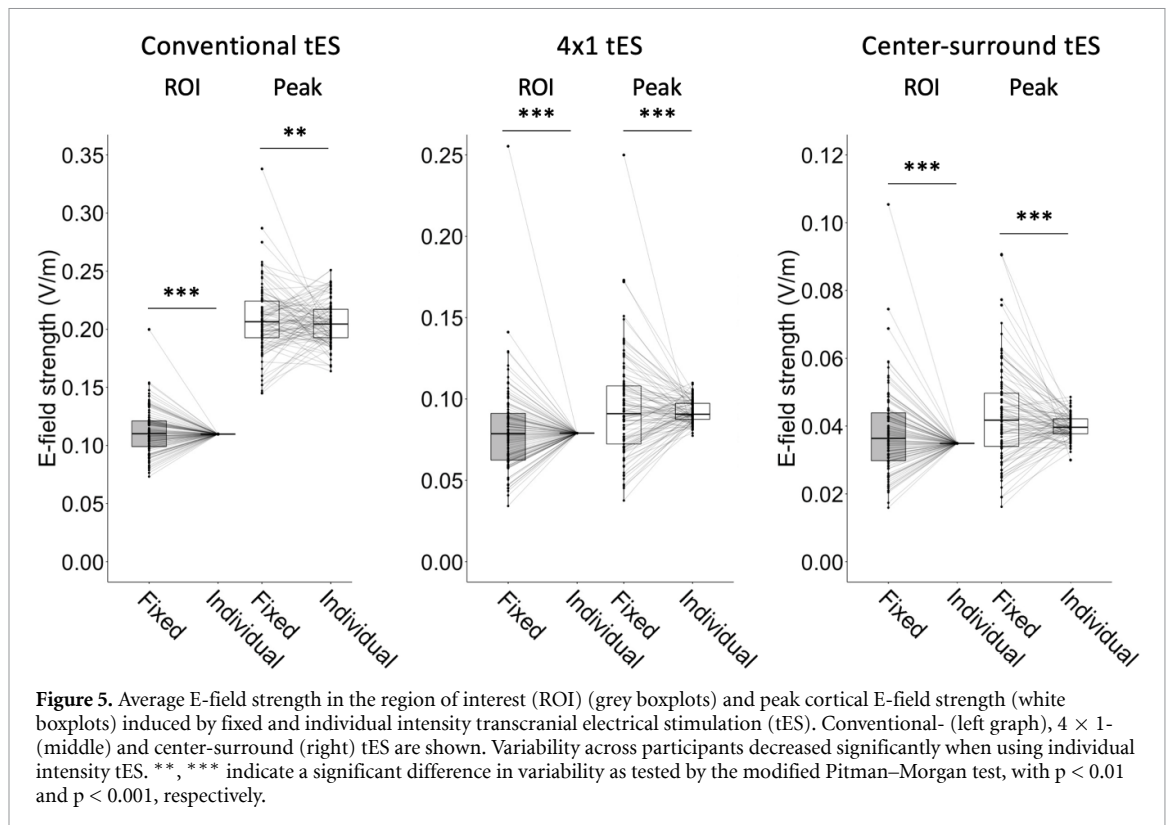


**Figure 4.** Qualitative comparison of electric fields (E-fields) induced by conventional-,  $4 \times 1$ - and center-surround transcranial electrical stimulation (tES). Each row shows one participant, namely the participant with the minimum (row 1), median (row 2) and maximum (row 3) E-field strength induced by fixed intensity tES across all 3 montages. Fixed intensity tES induces highly variable E-field strengths across participants while individual intensity tES [i.e. the 2-sample prospective dosing (2-SPED) approach] induces nearly identical E-field strengths across participants.



of  $0.035 \pm 0$  V/m. Variance in M1 E-field strengths induced by fixed tES (VC = 33.54%, range = 0.089 V/m) was significantly higher than variance induced by individualized tES (VC = 0%, range = 0 V/m),  $r_{98} = 1$ ,  $p < 0.001$  (figure 5).

Peak E-field strength induced by fixed and individualized tES was  $0.043 \pm 0.014$  V/m and  $0.040 \pm 0.003$  V/m, respectively. Variation was significantly higher as a result of fixed tES (VC = 32.49%, range = 0.075 V/m) versus individualized tES (VC = 8.61%, range = 0.019 V/m),  $r_{98} = 0.87$ ,  $<0.001$  (figure 5).

#### 4. Discussion

Here, we set out to establish the 2-SPED approach to reduce interindividual E-field strength variability. By doing so, we aimed to ameliorate the capacity of tES to instigate consistent neurophysiological and behavioral changes in the fields of basic and applied sciences. Specifically, we simulated three common tES montages in 289 healthy persons. In line with previous intracranial and computational studies, we found that E-field strengths induced by 1 mA tES remain well-below 0.5 V/m and are highly variable [13, 19, 43–45]. To illustrate the latter point, the highest ROI E-field strength induced by conventional M1–SO fixed intensity tES in a participant (0.200 V/m) was 177.78% higher than the lowest induced E-field strength (0.072 V/m). Furthermore, E-field strengths induced by fixed intensity  $4 \times 1$  tES were the most

variable (cf, figure 2 and table 2), which corroborates previous work stating that the enhanced focality of  $4 \times 1$  HD-tES comes at the cost of increased inter-individual variability [46]. The 2-SPED approach significantly reduced both ROI and peak E-field variability in all 3 tES montages. Moreover, individual stimulation intensity ranged between 0.309 and 2.307 mA across all individuals of sample 2 to produce the group average that 1 mA stimulation produces in sample 1. As such, it remained well-within the proposed tES intensity safety limits [47, 48].

While the current simulations were restricted to 1 mA tES, the implications of our findings are not. Our results are extrapolatable to other stimulation intensities such as 2 and 4 mA tES due to the linear ohmic nature of tES E-field generation and the linearity of the 2-SPED method [21, 44]. For instance, by multiplying all E-field strength (V/m) values by 2, one acquires the values that 2 mA tES simulations would obtain. This would not affect the statistical results given that all values would be multiplied by the same factor.

Several methods have been developed to diminish interindividual tES E-field strength variability via stimulation intensity individualization, with none of the approaches being empirically tested via *in-vivo*, physical, studies. For instance, Evans *et al* introduced Dose-Controlled tES, which reverse-calculates an individual stimulation intensity [19]. Another approach uses the transcranial electrical stimulation (TES) induced motor threshold for individualization

[21]. Finally, Antonenko *et al* individualized stimulation intensity to obtain more uniform E-field strengths across individuals through head circumference measurements [49]. Although all of these methods yield merit, they are subject to several limitations which limit their implementability. For instance, practical implementation of Dose-Controlled tES is hindered by its need to scan an entire study sample, prior to being able to individualize tES. By facilitating prospective use (i.e. one could scan the first participant and do individualized tES on the same day), 2-SPED solves this. Also, TES induced motor threshold individualization is limited by its inability to measure E-field strength and by the fact that TES motor threshold determination can be intolerable for some individuals. Finally, the head circumference individualization approach only explains  $\sim 25\%$  of the variance of E-field strengths. Therefore, the approach still permits a substantial degree of interindividual E-field strength variability. As 2-SPED addresses these limitations, implementation is more feasible. This focus on feasibility compliments the necessity of the scientific field to start empirically researching the effect of individualized intensity tES on neurophysiological and behavioral parameters.

Conceptualization and validation of our novel 2-SPED tES approach facilitates the use of the reverse-calculation method in a prospective, *in-vivo* manner. Results indicate that it is possible to calculate a stable group average E-field value from a dataset (S1), and use the obtained value for individualisation of tES intensity in a second sample (S2), that is yet to be recruited. As such, our 2-SPED approach allows researchers to determine and implement an informed group average E-field strength for prospective dosing using reverse-calculation E-field modeling. However, it is important to note that the group average E-field strength of S1 is not necessarily the optimal E-field strength to induce maximal physiological and/or behavioral effects and is limited by the tES intensities applied to date (typically 2 mA or below). Several studies have associated higher E-field strengths with greater neurophysiological and behavioral improvements, either directly or indirectly (through higher stimulation intensities which give rise to higher E-field strengths) [10–13, 15, 50, 51]. At first glance, this seems to imply that inducing high E-field strengths is more advantageous than inducing group average E-field strengths. Although this might hold true, one should be cautious portraying the relationship between tES induced E-field strength and neurophysiological/behavioral effects as unilinear. First, this assumption does not consider factors such as stimulation duration, despite the fact that stimulation duration may alter the longevity of the induced effects and even influences the direction of tES-instigated effects [52, 53]. Second, this hypothesis

contradicts the results of Batsikadze *et al* and Weller *et al*, who demonstrated that higher tES stimulation intensities (i.e. with higher induced E-fields) can shift the direction of neural effects and can reduce the effectiveness of tES in terms of cognitive improvements [22, 54]. Third, as most tES studies have delivered stimulation at intensities of 2 mA or lower, the dose-response curve has not yet been fully elucidated. It could be that a certain point, the potential benefit of increasing stimulation intensity ( $\sim$ E-field strength) reaches a plateau. From this point onwards, further increasing stimulation intensity will only result in elevated participant discomfort and should therefore be avoided. Thus, the potential benefit of using 2-SPED and basing individualized E-field dosing on group average E-fields is that it theoretically ensures that participants are neither under- nor over-stimulated, as is the case in conventional fixed intensity tES.

To advance the field of noninvasive brain stimulation, it is of vital importance that future studies set out to unravel the optimal E-field strength through dosage titration. While previous studies have aimed to achieve this through comparisons of different stimulation intensities and/or post-hoc correlations linking induced E-field strength to the outcome measure, we propose that the 2-SPED approach could be equally valuable. Implementation of 2-SPED would ensure that all participants receive nearly-identical E-fields in the targeted region. Thus, the risk of underdosing certain participants would be minimized. In parallel, by reducing E-field variability inherent to fixed-intensity tES, 2-SPED allows researchers to better isolate the impact of different tES parameters that also determine tES effectiveness, without conflating these changes with different inter-individual E-fields. Lastly, in contrast to post-hoc correlational studies linking E-field strength to outcome measures, the 2-SPED approach is capable of delivering causal evidence for the presence of an optimal E-field strength. In doing so, it can also confirm the importance of E-field strength as a vital parameter of tES, and the relevance of computational E-field dosimetry.

A potential avenue for a future study aiming to achieve these goals could be to first determine a group average E-field strength in an available participant cohort (or use a group average reported here, if participant and tES characteristics are corresponding) and prospectively use reverse-calculations to induce  $0.5\times$ ,  $1\times$ , and  $2\times$  the group average E-field in a second population, comparing neurophysiological, behavioral and/or clinical effects of the different E-fields. If an optimal E-field strength were to be identified, the reverse-calculation method could be used to induce this E-field strength in all participants, irrespective of anatomy.



## 5. Limitations

The current work was subject to several limitations that should be considered.

First and foremost, while there is strong evidence in favor of the link between E-field strength and tES outcome [8–15], factors such as tES duration, tES timing (i.e. online versus offline administration), brain state and applied current direction also determine tES effectiveness [18, 55–57]. Given that these factors are not individualized via 2-SPED, one can expect 2-SPED to not entirely mitigate tES outcome variability. However, given that 2-SPED controls for the important variable E-field strength, it provides a more controlled approach to disentangle these other factors in the future. For instance, investigating how tES duration influences tES effectiveness becomes much more straightforward when one is certain that all participants receive the same E-field strength at the neural ROI. Moreover, as there is reason to believe that E-field strength and tES duration are non-linearly related, the appeal of inducing uniform E-field strengths to investigate tES duration in a more controlled manner increases even further [58, 59].

Second, 2-SPED has not yet been validated *in-vivo*. Although the advantages of 2-SPED in computational models and its feasibility are promising, empirical evidence via neurophysiological and behavioral experiments, is the much-needed next step prior to implementing 2-SPED in routine practice. This could be a promising avenue for future studies.

Third, our approach assumes that E-field simulations are accurate. While most intracranial recordings support this assumption [43, 44, 60, 61], misestimations have been observed [60]. Thus, when applying the 2-SPED method in an experimental setting, one should be aware that there might be some individuals who do not receive the same E-field strength as the rest of the group due to misestimations. Nevertheless, 2-SPED is compatible with updates to E-field methodology. Future improvements in E-field simulation accuracy will lead to a decreased number of misestimations and will further ameliorate the use of 2-SPED. Furthermore, despite some misestimations, the 2-SPED approach should still significantly improve E-field homogeneity across persons, on average. On a similar note, simulations are dependent on MRI-scan parameters. Therefore, future work should aim to acquire scans in line with the current best-practice, unless a strong rationale is present to deviate from them [27–29]. Likewise, the accuracy of the simulations, and thus by extension 2-SPED, depends on the accuracy of tissue conductivity values. Here, we used standard conductivity values, which have been used by a previous tES modeling validation study [60]. Nevertheless, it is important to acknowledge that tissue conductivity uncertainty impacts the

accuracy of E-field simulations [62]. Incorrect tissue conductivity values in some individuals could lead to misestimations by the 2-SPED approach, which, in turn, could cause 2-SPED to fail its goal of inducing uniform E-fields in these individuals.

Fourth and finally, we opted to use SimNIBS—headreco (SPM12 + CAT12) for modeling and segmentation, although several other approaches are available (i.e. CHARM, ROAST and SimNIBS—mri2mesh) [33, 34, 63]. While an elaborate comparison of these approaches is beyond the scope of our work and has already been conducted [33, 63], it is important to emphasize that post-segmentation processing in SimNIBS—headreco enforces all tissue layers to be fully enclosed by the subsequent tissue layer, prioritizing continuity of layers at the cost of anatomical accuracy. On the other hand, the SimNIBS—headreco approach enables the inclusion of accurate surface segmentations of the brain pial surfaces into the model building process, which is not possible via approaches that rely only on the anatomically coarser results of volume segmentation methods. Moreover, SimNIBS 3 creates one homogenous bone tissue layer with a single, adjusted, conductivity value. Although the anatomically correct, three-layered bone tissue model (i.e. spongy bone enclosed by compact bone on the interior and exterior side of the skull) has been incorporated in some head models, a single bone layer with adjusted conductivity value yields similar E-field strength-related results, is less computationally demanding, and is considerably more often used in the E-field modeling literature [29, 43, 44, 60–62, 64, 65].

## 6. Conclusion

Through three commonly used tES montages, we demonstrated that the 2-SPED approach enables prospective individualization of tES intensity to induce uniform E-field strengths in a population. In line with previous literature, we demonstrated that individual intensity tES produces identical E-fields in the ROI across participants, as well as significantly less variable peak cortical E-fields. Given that E-field strength is a cardinal physical agent of tES, 2-SPED yields great scientific promise. It can be implemented to unravel the neural effects underlying tES, and to investigate other determinants of tES effectiveness, such as current direction and stimulation duration, while controlling for a large source of variability (i.e. E-field strength).

## Data availability statement

The data that support the findings of this study are available from the corresponding author upon reasonable request.

## Acknowledgments

This work was supported by the Special Research Fund (BOF) of Hasselt University (BOF20KP18), an NIH NINDS F31 NRSA grant (Principal Investigator: Kevin A Caulfield; 1F31NS126019-01), the Lundbeck foundation (Axel Thielscher; Grant R313-2019-622) and the European Union's Horizon 2020 research and innovation program (Michael A Nitsche; No. 101017716). Data were provided by the Human Connectome Project, WU-Minn Consortium (Principal Investigators: David Van Essen and Kamil Ugurbil; 1U54MH091657) funded by the 16 NIH Institutes and Centers that support the NIH Blueprint for Neuroscience Research; and by the McDonnell Center for Systems Neuroscience at Washington University.

## Conflict of interest

We confirm that all authors have no known conflicts of interest associated with this publication and there has been no financial or personal relationship with other people/organizations that could inappropriately influence this work.

## ORCID iDs

Sybre Van Hoornweder  <https://orcid.org/0000-0002-0325-8950>

Kevin A Caulfield  <https://orcid.org/0000-0001-8268-4204>

Axel Thielscher  <https://orcid.org/0000-0002-4752-5854>

Raf L J Meesen  <https://orcid.org/0000-0002-7938-3758>

## References

- [1] Nitsche M A and Paulus W 2000 Excitability changes induced in the human motor cortex by weak transcranial direct current stimulation *J. Physiol.* **527** 633–9
- [2] Bikson M, Inoue M, Akiyama H, Deans J K, Fox J E, Miyakawa H and Jefferys J G R 2004 Effects of uniform extracellular DC electric fields on excitability in rat hippocampal slices *in vitro* *J. Physiol.* **557** 175–90
- [3] Battleday R M, Muller T, Clayton M S and Cohen Kadosh R 2014 Mapping the mechanisms of transcranial alternating current stimulation: a pathway from network effects to cognition *Frontiers Psychiatry* **5** 162
- [4] Reed T and Cohen Kadosh R 2018 Transcranial electrical stimulation (tES) mechanisms and its effects on cortical excitability and connectivity *J. Inherit. Metab. Dis.* **41** 1123–30
- [5] Hnmbmwaj K 2019 *Practical Guide to Transcranial Direct Current Stimulation: Principles, Procedures and Applications* (Cham: Springer) (<https://doi.org/10.1007/978-3-319-95948-1>)
- [6] Laakso I, Tanaka S, Koyama S, De Santis V and Hirata A 2015 Inter-subject variability in electric fields of motor cortical tDCS *Brain Stimul.* **8** 906–13
- [7] Wiethoff S, Hamada M and Rothwell J C 2014 Variability in response to transcranial direct current stimulation of the motor cortex *Brain Stimul.* **7** 468–75
- [8] Laakso I, Mikkonen M, Koyama S, Hirata A and Tanaka S 2019 Can electric fields explain inter-individual variability in transcranial direct current stimulation of the motor cortex? *Sci. Rep.* **9** 626
- [9] Leunissen I, Van Steenkiste M, Heise K-F, Monteiro T S, Dunovan K, Mantini D, Coxon J P and Swinnen S P 2022 Effects of beta-band and gamma-band rhythmic stimulation on motor inhibition *iScience* **25** 104338
- [10] Nandi T et al 2022 tDCS induced GABA change is associated with the simulated electric field in M1, an effect mediated by grey matter volume in the MRS voxel *Brain Stimul.* **15** 1153–62
- [11] Zanto T P, Jones K T, Ostrand A E, Hsu W-Y, Campusano R and Gazzaley A 2021 Individual differences in neuroanatomy and neurophysiology predict effects of transcranial alternating current stimulation *Brain Stimul.* **14** 1317–29
- [12] Kasten F H, Duecker K, Maack M C, Meiser A and Herrmann C S 2019 Integrating electric field modeling and neuroimaging to explain inter-individual variability of tACS effects *Nat. Commun.* **10** 5427
- [13] Caulfield K A, Indahlstari A, Nissim N R, Lopez J W, Fleischmann H H and Woods A J 2020 Electric field strength from prefrontal transcranial direct current stimulation determines degree of working memory response: a potential application of reverse-calculation modeling? *Neuromodulation* **25** 578–87
- [14] Mikkonen M, Laakso I, Sumiya M, Koyama S, Hirata A and Tanaka S 2018 TMS motor thresholds correlate with TDCS electric field strengths in hand motor area *Front. Neurosci.* **12** 426
- [15] Wischniewski M, Mantell K E and Opitz A 2021 Identifying regions in prefrontal cortex related to working memory improvement: a novel meta-analytic method using electric field modeling *Neurosci. Biobehav. Rev.* **130** 147–61
- [16] Liu A et al 2018 Immediate neurophysiological effects of transcranial electrical stimulation *Nat. Commun.* **9** 5092
- [17] Preisig B and Hervais-Adelman A 2022 The predictive value of individual electric field modeling for transcranial alternating current stimulation induced brain modulation *Front. Cell. Neurosci.* **16** 818703
- [18] Evans C, Zich C, Lee J S A, Ward N and Bestmann S 2022 Inter-individual variability in current direction for common tDCS montages *Neuroimage* **260** 119501
- [19] Evans C, Bachmann C, Lee J S A, Gregoriou E, Ward N and Bestmann S 2020 Dose-controlled tDCS reduces electric field intensity variability at a cortical target site *Brain Stimul.* **13** 125–36
- [20] Caulfield K A, Badran B W, Li X, Bikson M and George M S 2020 Can transcranial electrical stimulation motor threshold estimate individualized tDCS doses over the prefrontal cortex? Evidence from reverse-calculation electric field modeling *Brain Stimul.* **13** 1150–2
- [21] Caulfield K A, Badran B W, DeVries W H, Summers P M, Kofmehl E, Li X, Borckardt J J, Bikson M and George M S 2020 Transcranial electrical stimulation motor threshold can estimate individualized tDCS dosage from reverse-calculation electric-field modeling *Brain Stimul.* **13** 961–9
- [22] Weller S, Nitsche M A and Plewnia C 2020 Enhancing cognitive control training with transcranial direct current stimulation: a systematic parameter study *Brain Stimul.* **13** 1358–69
- [23] Heise K-F, Monteiro T S, Leunissen I, Mantini D and Swinnen S P 2019 Distinct online and offline effects of alpha and beta transcranial alternating current stimulation (tACS) on continuous bimanual performance and task-set switching *Sci. Rep.* **9** 3144
- [24] Saturnino G B, Madsen K H, Siebner H R and Thielscher A 2017 How to target inter-regional phase synchronization with dual-site transcranial alternating current stimulation *Neuroimage* **163** 68–80
- [25] Minhas P, Bansal V, Patel J, Ho J S, Diaz J, Datta A and Bikson M 2010 Electrodes for high-definition

- transcutaneous DC stimulation for applications in drug delivery and electrotherapy, including tDCS *J. Neurosci. Methods* **190** 188–97
- [26] Van Essen D C et al 2012 The Human Connectome Project: a data acquisition perspective *Neuroimage* **62** 2222–31
- [27] Van Hoornweder S, Meesen R and Caulfield K A 2022 On the importance of using both T1-weighted and T2-weighted structural magnetic resonance imaging scans to model electric fields induced by non-invasive brain stimulation in SimNIBS *Brain Stimul.* **15** 641–4
- [28] Van Hoornweder S, Meesen R L J and Caulfield K A 2022 Accurate tissue segmentation from including both T1-weighted and T2-weighted MRI scans significantly affect electric field simulations of prefrontal but not motor TMS *Brain Stimul.* **15** 942–5
- [29] Nielsen J D, Madsen K H, Puonti O, Siebner H R, Bauer C, Madsen C G, Saturnino G B and Thielscher A 2018 Automatic skull segmentation from MR images for realistic volume conductor models of the head: assessment of the state-of-the-art *Neuroimage* **174** 587–98
- [30] Friston K J 2007 *Statistical Parametric Mapping: The Analysis of Functional Brain Images* (Amsterdam/Boston: Elsevier/Academic)
- [31] Gaser C and Dahnke R 2016 CAT-A computational anatomy toolbox for the analysis of structural MRI data (<https://doi.org/10.1101/2022.06.11.495736>)
- [32] Puonti O, Saturnino G B, Madsen K H and Thielscher A 2020 Value and limitations of intracranial recordings for validating electric field modeling for transcranial brain stimulation *Neuroimage* **208** 116431
- [33] Huang Y, Datta A, Bikson M and Parra L C 2019 Realistic volumetric-approach to simulate transcranial electric stimulation—ROAST—a fully automated open-source pipeline *J. Neural. Eng.* **16** 056006
- [34] Thielscher A, Antunes A and Saturnino G B 2015 Field modeling for transcranial magnetic stimulation: a useful tool to understand the physiological effects of TMS? *2015 37th Annual Int. Conf. IEEE Engineering in Medicine and Biology Society (EMBC)* pp 222–5
- [35] Wagner T A, Zahn M, Grodzinsky A J and Pascual-Leone A 2004 Three-dimensional head model Simulation of transcranial magnetic stimulation *IEEE Trans. Biomed. Eng.* **51** 1586–98
- [36] Opitz A, Paulus W, Will S, Antunes A and Thielscher A 2015 Determinants of the electric field during transcranial direct current stimulation *Neuroimage* **109** 140–50
- [37] Saturnino G B, Antunes A and Thielscher A 2015 On the importance of electrode parameters for shaping electric field patterns generated by tDCS *Neuroimage* **120** 25–35
- [38] Mayka M A, Corcos D M, Leurgans S E and Vaillancourt D E 2006 Three-dimensional locations and boundaries of motor and premotor cortices as defined by functional brain imaging: a meta-analysis *Neuroimage* **31** 1453–74
- [39] Schönbrodt F D and Perugini M 2013 At what sample size do correlations stabilize? *J. Res. Pers.* **47** 609–12
- [40] RStudio Team 2020 *RStudio: Integrated Development for R*. PBC (Boston, MA: Rstudio)
- [41] R Core Team 2021 *R: A Language And Environment For Statistical Computing* (Vienna: R Foundation for Statistical Computing)
- [42] McCulloch C E 1987 Tests for equality of variances with paired data *Commun. Stat.-Theory Methods* **16** 1377–91
- [43] Huang Y, Liu A A, Lafon B, Friedman D, Dayan M, Wang X, Bikson M, Doyle W K, Devinsky O and Parra L C 2017 Measurements and models of electric fields in the *in vivo* human brain during transcranial electric stimulation *Elife* **6** e18834
- [44] Opitz A et al 2016 Spatiotemporal structure of intracranial electric fields induced by transcranial electric stimulation in humans and nonhuman primates *Sci. Rep.* **6** 31236
- [45] Chhatbar P Y, Kautz S A, Takacs I, Rowland N C, Revuelta G J, George M S, Bikson M and Feng W 2018 Evidence of transcranial direct current stimulation-generated electric fields at subthalamic level in human brain *in vivo Brain Stimul.* **11** 727–33
- [46] Mikkonen M, Laakso I, Tanaka S and Hirata A 2020 Cost of focality in TDCS: interindividual variability in electric fields *Brain Stimul.* **13** 117–24
- [47] Bikson M, Datta A and Elwassif M 2009 Establishing safety limits for transcranial direct current stimulation *Clin. Neurophysiol.* **120** 1033–4
- [48] Chhatbar P Y, Chen R, Deardorff R, Dellenbach B, Kautz S A, George M S and Feng W 2017 Safety and tolerability of transcranial direct current stimulation to stroke patients—a phase I current escalation study *Brain Stimul.* **10** 553–9
- [49] Antonenko D, Grittner U, Puonti O, Flöel A and Thielscher A 2021 Estimation of individually induced e-field strength during transcranial electric stimulation using the head circumference *Brain Stimul.* **14** 1055–8
- [50] Suen P J C et al 2021 Association between tDCS computational modeling and clinical outcomes in depression: data from the ELECT-TDCS trial *Eur. Arch. Psychiatry Clin. Neurosci.* **271** 101–10
- [51] Cuypers K, Leenus D J F, van den Berg F E, Nitsche M A, Thijs H, Wenderoth N and Meesen R L J 2013 Is motor learning mediated by tDCS intensity? *PLoS One* **8** e67344
- [52] Monte-Silva K, Kuo M F, Hessenthaler S, Fresnoza S, Liebetanz D, Paulus W and Nitsche M A 2013 Induction of late LTP-like plasticity in the human motor cortex by repeated non-invasive brain stimulation *Brain Stimul.* **6** 424–32
- [53] Nitsche M A and Paulus W 2001 Sustained excitability elevations induced by transcranial DC motor cortex stimulation in humans *Neurology* **57** 1899–901
- [54] Batsikadze G, Moliadze V, Paulus W, Kuo M F and Nitsche M A 2013 Partially non-linear stimulation intensity-dependent effects of direct current stimulation on motor cortex excitability in humans *J. Physiol.* **591** 1987–2000
- [55] Van Hoornweder S, Vanderzande L, Bloemers E, Verstraelen S, Depestele S, Cuypers K, Dun K V, Strouwen C and Meesen R 2021 The effects of transcranial direct current stimulation on upper-limb function post-stroke: a meta-analysis of multiple-session studies *Clin. Neurophysiol.* **132** 1897–918
- [56] Hassanzahraee M, Nitsche M A, Zoghi M and Jaberzadeh S 2020 Determination of anodal tDCS duration threshold for reversal of corticospinal excitability: an investigation for induction of counter-regulatory mechanisms *Brain Stimul.* **13** 832–9
- [57] Li L M, Violante I R, Leech R, Ross E, Hampshire A, Opitz A, Rothwell J C, Carmichael D W and Sharp D J 2019 Brain state and polarity dependent modulation of brain networks by transcranial direct current stimulation *Hum. Brain Mapp.* **40** 904–15
- [58] Ghasemian-Shirvan E, Mosayebi-Samani M, Farnad L, Kuo M F, Meesen R L J and Nitsche M A 2022 Age-dependent non-linear neuroplastic effects of cathodal tDCS in the elderly population: a titration study *Brain Stimul.* **15** 296–305
- [59] Mosayebi Samani M, Agboada D, Jamil A, Kuo M-F and Nitsche M A 2019 Titrating the neuroplastic effects of cathodal transcranial direct current stimulation (tDCS) over the primary motor cortex *Cortex* **119** 350–61
- [60] Opitz A, Yeagle E, Thielscher A, Schroeder C, Mehta A D and Milham M P 2018 On the importance of precise electrode placement for targeted transcranial electric stimulation *Neuroimage* **181** 560–7
- [61] Wang M, Feng T, Jiang H, Zhu J, Feng W and Chhatbar P Y 2022 *In vivo* measurements of electric fields during cranial electrical stimulation in the human brain *Front. Hum. Neurosci.* **16** 829745
- [62] Saturnino G B, Thielscher A, Madsen K H, Knösche T R and Weise K 2019 A principled approach to conductivity

- uncertainty analysis in electric field calculations *Neuroimage* **188** 821–34
- [63] Puonti O, Van Leemput K, Saturnino G B, Siebner H R, Madsen K H and Thielscher A 2020 Accurate and robust whole-head segmentation from magnetic resonance images for individualized head modeling *Neuroimage* **219** 117044
- [64] Cho J-H, Vorwerk J, Wolters C H and Knösche T R 2015 Influence of the head model on EEG and MEG source connectivity analyses *Neuroimage* **110** 60–77
- [65] Antonakakis M, Schrader S, Aydin Ü, Khan A, Gross J, Zervakis M, Rapp S and Wolters C H 2020 Inter-subject variability of skull conductivity and thickness in calibrated realistic head models *Neuroimage* **223** 117353